Article

Not peer-reviewed version

Environmental Chamber Characterization of an Ice Detection Sensor for Aviation Using Graphene and PEDOT:PSS

Dario Farina , Marco Mazio , Hatim Machrafi * , Patrick Queeckers , Carlo Saverio Iorio

Posted Date: 25 March 2024

doi: 10.20944/preprints202403.1444.v1

Keywords: Ice Formation; Aircraft Ice Detection; Hazard Management; Graphene Sensors; In-Flight Safety Technology; Real-time Ice Monitoring; Resistance Signal Analysis; Pedot:PSS; Climatic chamber

 doi:10.20944/preprints202403.1444.v1

Article

Environmental Chamber Characterization of an Ice Detection Sensor for Aviation Using Graphene and PEDOT:PSS

Dario Farina [1], Marco Mazio [2], Hatim Machrafi [1,3,*], Patrick Queeckers [1] and Carlo Saverio Iorio [1]

[1] Centre for Research and Engineering in Space Technologies (CREST), Department of Aero-Thermo-Mechanics, Université libre de Bruxelles
[2] Department of Industrial Engineering University Federico II of Naples
[3] UFR Physique, Sorbonne Université, Paris, France
* Correspondence: hatim.machrafi@ulb.be

Abstract: In the context of improving aircraft safety, this work focuses on creating and testing in an environmental chamber a graphene-based ice detecting system. The research is driven by the need for more accurate and efficient ice detection methods, crucial in mitigating in-flight icing hazards. The methodology employed involves testing flat graphene-based sensors in a controlled environment, simulating a variety of climatic conditions that could be experienced in an aircraft during its entire flight. The environmental chamber enabled precise manipulation of temperature and humidity levels, thereby providing a realistic and comprehensive test bed for sensor performance evaluation. The results were significant, revealing the graphene sensors' heightened sensitivity and rapid response to the subtle changes in environmental conditions, especially the critical phase transition from water to ice. This sensitivity is the key to detecting ice formation at its onset, a critical requirement for aviation safety. The study concludes that graphene-based sensors, tested under varied and controlled atmospheric conditions, exhibit a remarkable potential in enhancing ice detection systems for aircraft. Their lightweight, efficient and highly responsive nature makes them a superior alternative to traditional ice detection technologies, paving the way for more advanced and reliable aircraft safety solutions.

Keywords: aerospace icing prevention; risk mitigation in aviation; graphene-based sensors; dynamic ice sensing; de-icing; conductive polymer applications; smart sensors; PEDOT:PSS Polymers; 2D materials; micromachines

1. Introduction

The challenge of detecting ice during a flight in aviation has been a focal point of research due to its critical implications for flight safety, efficiency, and performance [1]. This phenomenon, a significant challenge across various flight conditions, occurs not only when supercooled water droplets in the atmosphere freeze upon contact with an aircraft's surface but also under a range of atmospheric conditions that facilitate ice formation. Ice can accumulate on aircraft surfaces through different mechanisms, including the impact of supercooled droplets, the freezing of rain upon contact, and the deposition of water vapor into ice in cold, dry conditions. Such conditions are most prevalent in clouds or areas of precipitation at temperatures below 0°C, but can also arise in clear air when moisture levels are high, and temperatures are conducive to icing. Ice formation on an aircraft disrupts the smooth flow of air across the wing surfaces and control elements, significantly altering aerodynamic properties. This leads to increased drag and reduced lift, which can compromise the aircraft's ability to maintain altitude and speed. Additionally, ice adds considerable weight, further diminishing performance and efficiency. The impact on control surfaces and propulsion systems can also severely limit a pilot's ability to maneuver and control the aircraft, posing significant risks during critical phases of flight such as takeoff and landing [2,3]. In response, the development of ice detection systems has become a key area in aviation technology. Traditional systems, ranging from mechanical methods to thermal and optical methods, have provided foundational information, but often face limitations in terms of response time, sensitivity, and applicability under diverse flight conditions [5,6].

 doi:10.20944/preprints202403.1444.v1

Recent advancements in material science have ushered in a new era of potential solutions, with graphene-based technologies at the forefront [7,8]. Graphene's exceptional conductivity, flexibility, and strength make it an ideal candidate for sensitive and accurate ice detection. Studies have shown promising results in utilizing graphene's properties for real-time ice formation detection [9].

One promising advancement in ice detection systems is the development of an aircraft sensor fault detection system based on the Steady-State Least Mean Squares (LMS) algorithm, which enhances the reliability of sensor networks in aviation by efficiently detecting and mitigating Byzantine attacks within wireless sensor networks [10]. Additionally, the exploration of aviation sensor performance evaluation methodologies has provided valuable insights into improving sensor reliability and effectiveness in challenging aviation environments, paving the way for more accurate and reliable ice detection technologies [11].

Micro-electromechanical systems (MEMS) technology has been widely explored for ice detection in aviation. Varadan et al. [12] provide an overview of MEMS-based sensors and their potential applications in smart structures and systems. The authors discuss the advantages of MEMS technology, including their small size, low power consumption, and high sensitivity, which make them ideal for ice detection in aviation. However, the paper also highlights the challenges and limitations of MEMS-based sensors, such as their susceptibility to environmental factors and the need for proper calibration and testing.

Another interesting study is the work by Strijhak et al. [13], which presents a neural network-based approach for predicting ice shapes on airfoils using computational fluid dynamics simulations. The researchers trained a neural network using data from iceFoam simulations to predict the ice shape on an airfoil under various icing conditions. The results of the study show that the neural network approach is able to accurately predict the ice shape with a high degree of accuracy, demonstrating the potential of this approach for enhancing ice detection and mitigation in aviation.

Despite these advances, the field continues to face challenges. There exists a spectrum of hypotheses on the most effective and practical approach to ice detection. The divergence lies mainly in balancing the sensitivity, reliability, and cost effectiveness of the systems in varying environmental conditions [14,15].

The purpose of this research is to critically evaluate the performance of graphene-based sensors within an environmental chamber, designed to simulate a range of atmospheric conditions pertinent to ice formation. This approach offers a novel perspective on understanding the capabilities and limitations of graphene sensors compared to existing technologies. The results are expected to contribute significantly to the current understanding of ice detection technologies, providing valuable insight for future advancements.

In summary, this research not only contributes to the ongoing discourse in the advanced detection of in-flight ice but also posits the potential of graphene-based technology as a transformative solution in enhancing aircraft safety. Our graphene-based sensor, utilizing PEDOT:PSS, is primarily aimed at aviation safety, offering real-time detection of ice on aircraft surfaces. Beyond aviation, it has potential applications in telecommunications and road transport. Its accuracy, however, may be influenced by extreme environmental conditions, with constraints performance near 0°C. This innovation promises significant advancements in ice detection technologies across various industries.

2. Experimental Setup and Methodology

In this section, we describe the development of the sensors used for the experiments in the ice detection system. The sensor comprises a sensing part responsible for signal generation and a conductive part for signal transport to the data logger.

2.1. PEDOT:PSS a Conductive Polymer for Sensing

This study explores the use of PEDOT in thermoelectric devices used for ice detection, emphasizing its flexibility, eco-friendliness, and cost-effectiveness. Despite atmospheric sensitivity and

 doi:10.20944/preprints202403.1444.v1

moderate efficiency, doping with PEDOT:PSS improves conductivity through redox reactions, affecting its structure. PEDOT's excellent conductivity and stability, along with PEDOT:PSS's role as a mixed conductor, are crucial, although GOPS (3-glycidyloxypropyl)trimethoxysilane, often used to increase the stability of PEDOT:PSS, through crosslinking, may however lower conductivity due to its effects on the material's structural properties [16]. Its structure facilitates charge mobility, with humidity affecting charge transport modes. These findings are vital to state the possibility of using it in flight conditions [17,18]. The principle of ice detection by the sensor involves using PEDOT:PSS, a polymeric mixed ionic-electronic conductor, which displays a significant increase in electrical resistance during the phase transition from liquid water to solid ice. This change is attributed to the morphology and electronic transport in PEDOT being affected by the freezing event, as the absorbed water in the PSS-rich phase expands upon forming ice crystals.

2.2. Graphene-Based Sensors

Graphene is a single layer of carbon atoms arranged in a two-dimensional honeycomb lattice, known for its remarkable strength, flexibility, electrical, and thermal conductivity. Graphene's integration into 3D structures enhances sensing systems, offering low thermo-mechanical stress and easy incorporation into complex shapes [19]. Its exceptional conductivity increases operational efficiency in applications such as ice detection in aircraft, significantly reducing energy consumption. The compatibility of graphene with various materials, including polymers and fibers, broadens its application scope. The consistent low resistance of the material simplifies PEDOT:PSS resistance analysis, improving system evaluations. A particular graphene electrode configuration was chosen for its effectiveness in identifying ice, highlighting graphene's utility in innovative sensor configurations. This design, detailed in figures, showcases the integration and application of graphene electrodes within the detection system, emphasizing their dimensional precision and fabrication specifics, which are crucial for the sensor's performance. Our graphene-based sensor utilizes graphene's unique electrical properties, including sensitivity to changes in electrical conductivity and capacitance, to detect ice formation. When ice forms on the sensor's surface, it disrupts the charge distribution and electrical pathways of the graphene, a change that is rapidly detected and quantified for precise icing event identification

2.3. Sample Creation

For the sensing element, PEDOT:PSS is employed for its own hygroscopic properties, conductivity, water solubility, and elasticity [7].

The fabrication process for PEDOT:PSS (ratio of 1:2.5) sensing films involves the careful formulation of the polymer mixture, starting with Clevios PH1000 from Heraeus Holding GmbH (Leverkusen, Germany) was filtered through a 0.45 µm polyvinylidene fluoride (PVDF) filter, which is filtered for purity. GOPS is then integrated for mechanical stability, ensuring the films maintain their integrity upon exposure to moisture. This step is crucial for enhancing the longevity and reliability of the sensors under various environmental conditions. The solution is subjected to thorough mixing and sonication for 5-10 minutes to guarantee a homogeneous mixture, setting the stage for optimal film deposition. This method underscores the importance of precision in creating sensors that exhibit both high electronic and ionic conductivity, crucial for their functionality in detecting environmental changes such as ice formation. The interaction between the inherent conductive properties of the polymer and external factors such as humidity is a key consideration in the design and application of these sensing films, with the aim of leveraging their unique charge transport mechanisms for efficient and accurate sensing capabilities [7].

The capacity to absorb water is crucial for the detector's operation. The sensing element provides a signal by detecting changes in resistance as the absorbed water transitions from the liquid to the solid ice state. Graphene was produced as GS50-type graphene ribbons by NANESA SRL (Arezzo,

 doi:10.20944/preprints202403.1444.v1

Italy), with dimensions of 40 mm × 5 mm × 0.10 mm. In this research, GS50 denotes the graphene paper utilized as a crucial element of our sensor configuration [20].

Silicone rubber, also known as PDMS, trimmed to specific sizes, provides a pliable foundation crucial for integrating the system into an airfoil. Prepared graphene strips, cut to exact dimensions, form the conductive routes. Copper adhesive tape secures these strips, ensuring robust electrical linkages. A carefully placed droplet of PEDOT:PSS, applied through drop-casting, connects the strips, transforming them into a unified conductive route once it dries.

Following this, the samples undergo a 24-hour drying period at room temperature to guarantee the durability of the conductive link. The completed version of the sensor is illustrated in Figure 1. Resistance tests confirm the sensor's reliability prior to its use.

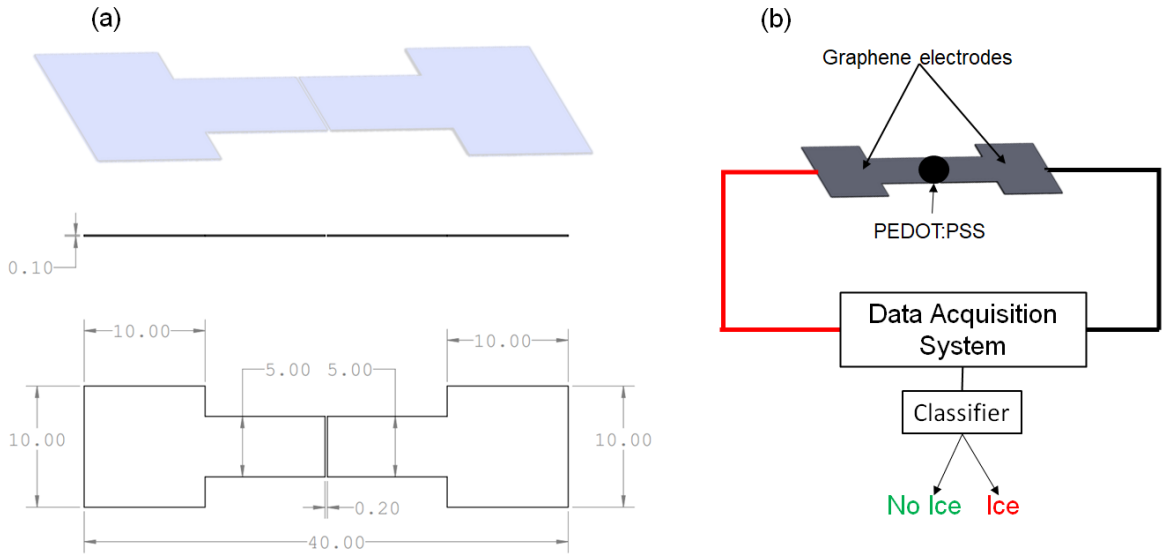

Figure 1. (**a**) Sketch of the electrodes engineered and utilized in all characterization studies. Measurements are depicted in millimeters. (**b**) The unified system featuring graphene electrodes, PEDOT:PSS detection layer, data gathering system, and interpretable output display.

The concluding phase entails attaching wires to the conductive copper tape, which acts as a bridge between the graphene and cables, and linking this setup to a data acquisition unit, the Agilent 34970A (Agilent Technologies, Santa Clara, CA, USA). This connection allows for the continuous observation and analysis of resistance, linking resistance changes to phase transitions caused by airflow. The finished sensors, as shown in Figure 1, are distinguished by their adaptability, compact size, and light construction. These attributes allow for their unobtrusive attachment to aircraft exteriors, permitting a collaborative sensor network for pinpoint ice detection. This method is in line with the broader objective of enhancing energy efficiency through focused de-icing, bolstered by accurate detection techniques. A critical aspect to highlight is the sensor's adaptability, offering the flexibility to modify its size according to the intended use area while maintaining its capabilities for detecting water and ice.

2.4. Environmental Chamber Setup

The experiments were carried out within a controlled environmental chamber built in our facilities (Université libre de Bruxelles, Bruxelles, Belgium). The environmental chamber allowed for the manipulation of the inside temperature, the temperature of the injected droplets and the humidity levels, closely replicating a range of climatic scenarios relevant to ice formation on an aircraft. This chamber served as a controlled test bed crucial for evaluating the performance of the graphene-based ice detection sensors.

 doi:10.20944/preprints202403.1444.v1

The schematic diagrams depict an environmental chamber designed for simulation, control, and monitoring of environmental conditions. The Figure 2a centers on the chamber itself, outfitted with temperature sensors type T and a top view camera JAI 500B for visual monitoring, and a side camera JAI 5000 for side camera view. Alongside, a cooling mechanism with distinct inlets and outlets was providing the capability for detailed temperature adjustments. A second thermal bath was supplying the capacities of temperature adjustment(between +1 °C and +40 °C) of the droplets injected.

The climate chamber consists of a cubic metal body cooled by a refrigerant fluid circulating within a serpentine of pipes arranged around the chamber walls. To enhance thermal insulation, the entire chamber is covered with 40 mm thick polyester that is 800 mm high.

A thermal bath is connected to the serpentine, enabling precise temperature control within the chamber. The chamber can maintain a minimum temperature of -20 °C, allowing for the simulation of a cryogenic environment.

Water is injected into the chamber through a syringe pump controlled by a LabView unit. This setup facilitates the injection of a defined volume of water in the form of small droplets. Typically, 24 µl droplets are released during experiments to study the effects of a specific quantity of water on PEDOT:PSS, which translates to an estimated diameter of approximately 5 millimeters. The pump mechanism is approximately 30 cm above the sample plate.

In the setup, T-type Copper-Constantan thermocouples are used.

Each sample is mounted on a Tec1-12715 Peltier element measuring (40x40x3.3) mm. This element operates on the Peltier effect, generating a temperature difference between its two sides when a voltage is applied. The cold side can reach temperatures below room temperature, allowing ice formation, and T_{cold} is the temperature measured on the cold side of the Peltier. A heat sink is attached to the hot side to rapidly dissipate heat.

To facilitate the melting of ice formed on the sensor after each experiment, a 60 Watt heater is employed.

Adjacent to the environmental chamber are an acquisition system and a circuit board, serving as the system's computational and control hub. The Figure 2c expands on this by showing an Arduino board connected to various components, including an LCD displaying temperature and humidity values, indicating a user interface for real-time data monitoring. The humidity level within the facility is controlled by activating a humidifier (to increase humidity) or turning on two small fans to circulate air and reduce humidity.

For data acquisition, the ice detector is connected to an Agilent 34970A (Agilent Technologies, Santa Clara, CA, USA) data logger, which reads three temperature values (two from thermocouples on chamber walls and one from the sensing element of the detector) and the internal resistance of the sample, including PEDOT, graphene strips, and electrical connections. This instrument combines precision measurement capabilities with flexible signal connections and is capable of logging and data acquisition. During the tests in the climate chamber, data are acquired at a frequency of 5 Hz.

Additional elements such as a humidifier and a heater coupled with a fan underscore the system's ability to manipulate both temperature and humidity levels within the chamber. Fans positioned around the chamber facilitate air circulation, essential for maintaining consistent conditions throughout the space.

 doi:10.20944/preprints202403.1444.v1

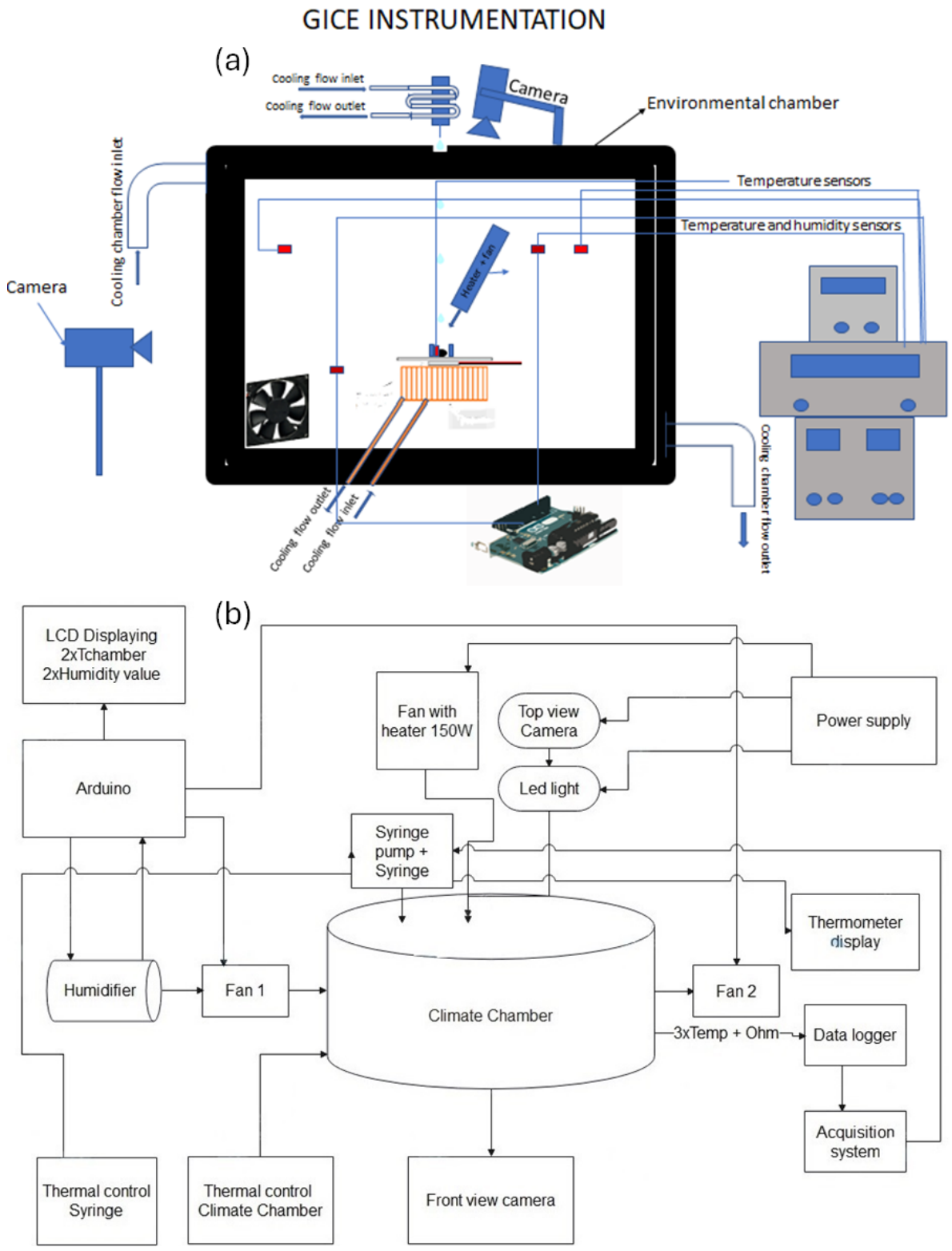

Figure 2. **(a)** Diagram of the setup. The environmental chamber is depicted with the main components. **(b)** Presents a schematic of the climate chamber setup used for ice detection experiments, featuring an Arduino-based control system, humidity and temperature regulation, and real-time monitoring capabilities via cameras and sensors.

 doi:10.20944/preprints202403.1444.v1

2.5. Experimental Procedure

The objective of the experiments is to create icing environments to study the signals generated by the ice detection system and to analyze how these signals change under varying external conditions, such as the chamber temperature. Such a study is crucial to characterize the detection technology, which will find its primary application in the subsequent wind tunnel tests conducted [**?**].

The experiment begins by setting the temperature parameters and the number of iterations. The acquisition system is started for video and data recording, followed by data acquisition. Water droplets are injected and cycles of heating and cooling occur.

When a droplet from the syringe was injected above Figure 3, it fell onto the sensing element of the sample and was absorbed by PEDOT. When the cold side reached a temperature below 0 °C, the water froze, and ice formed on the sample. After this process is measured and recorded, the ice was melted by increasing the temperature of the Peltier element or a fan, preparing for the next cycle.

The maximum temperature range achievable with the Peltier cell used was 60°C. The temperature was closely monitored using the thermocouples described above. The humidity level inside the chamber was maintained at a constant of 90%.

Figure 3. Example of drop injection (side view).

Table 1 provides a matrix of climatic chamber tests, indicating the range of minimum T_{cold} temperatures for each experiment along with the number of iterations. Experiments at higher temperatures were observed to require more time to form ice.

Table 1. Climatic Chamber Test Matrix

T cold (°C)	Number of iterations
-25 to -20	166
-20 to -15	45
-15 to -10	84
-10 to -5	80
-5 to 0	51

 doi:10.20944/preprints202403.1444.v1

Furthermore, the impact of chamber temperatures was evaluated, although most of the experiments were conducted at positive $T_{chamber}$ temperatures.

In Figure 4, a representative series of cycles executed is presented to illustrate the subtle influence of temperature variation on resistance, which pales compared to significant changes, of the order of kilo or mega ohms (KΩ), observed during ice formation, as will be discussed later. It is to be noted that a temperature sensor was strategically positioned directly above the PEDOT surface to precisely monitor temperature fluctuations upon droplet impact. The fluctuations observed in (T_{pedot}) are attributed to heat exchange phenomena, while abrupt resistance fluctuations are mainly attributed to the reduced conductivity of ice compared to water, a characteristic that becomes evident during phase transition [7,8]. In addition, the observed trend of increasing resistance with each cycle can be further explained by the gradual decrease in water volume on the sensor's surface, likely due to evaporation. This results in the resistance stabilizing at a higher value for each subsequent cycle, reflecting the lower conductivity as a result of the reduced water content. This complements the initial observation that while temperature variation subtly influences resistance, the more substantial changes are primarily attributed to the conductivity differences between ice and water during phase transitions.

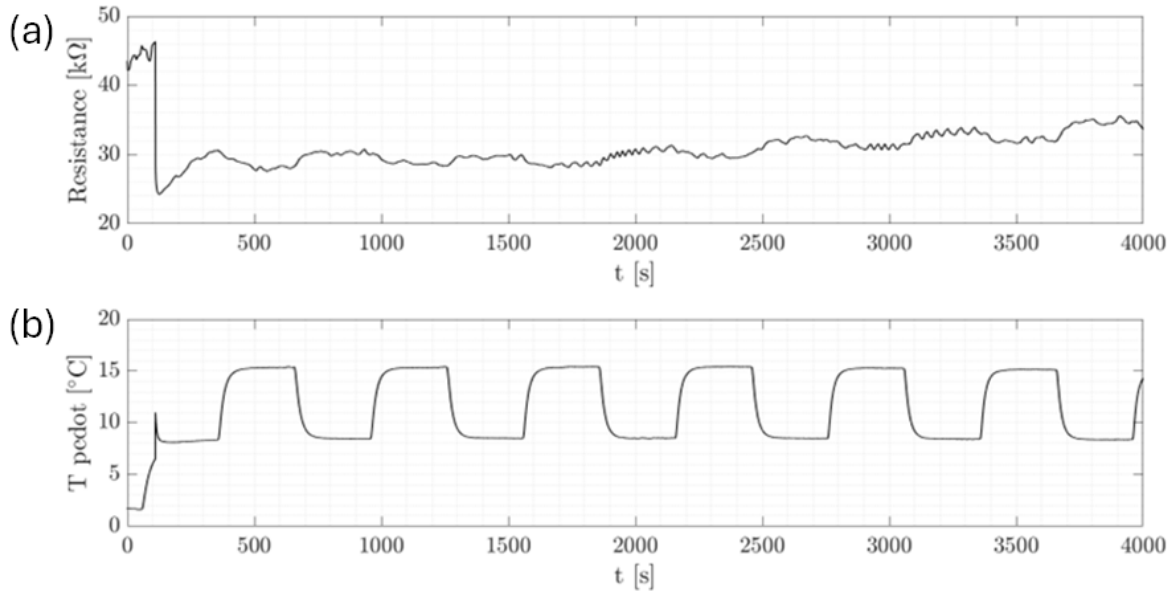

Figure 4. Temperature-controlled chamber experiment. Single drop. T_{cold} = 8 °C, $T_{chamber}$ = 15°C. (a) Resistance behavior. (b) Temperature behavior of the sensing element.

3. Results

The characterization of the ice detection system is performed by linking the changes in internal resistances to the phase changes in the water absorbed by the sensing element of the detector.

Each sample has a similar internal resistance (order of magnitude of 10^4 kΩ), eliminating the need to use a normalized resistance.

The volume of each drop is estimated at 24 µl, and the injected water is at ambient temperature. The cycles performed can be observed from the temperature trend provided by the thermocouple in contact with the sensing element.

The amplitude of signals and their dependence on chamber conditions are investigated. Figures show resistance and temperature patterns during droplet injection, ice formation, and ice melting.

Figure 5 displays the dynamic process of ice formation over three cycles, characterized by an initial drop in resistance and a rise in T_{pedot} values. This initial change is attributed to the impact of a water droplet. As time passes, resistance increases sharply as shown in the zoom of Figure 6, indicating the phase transition from liquid to solid as the droplet freezes. The cyclical pattern of these changes is consistent across the events, demonstrating the sensor's capability to detect and respond to successive

 doi:10.20944/preprints202403.1444.v1

icing conditions with high repeatability. Figures 7 and 8 show the same at different T_{cold}. It appears that the increase of resistance is lower as T_{cold} increases. The values of these resistance increases are shown in Table 2

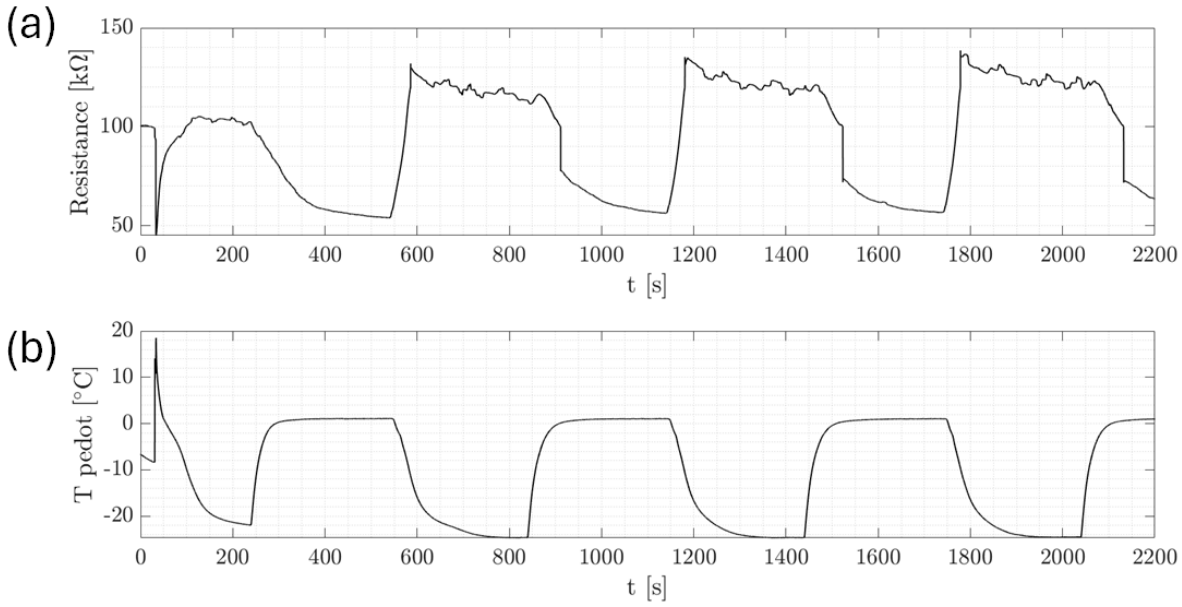

Figure 5. Characteristic water and ice signals at T_{cold} = -25°C, $T_{chamber}$ = 15°C. (a) Resistance behavior. (b) Temperature behavior of the sensing element.

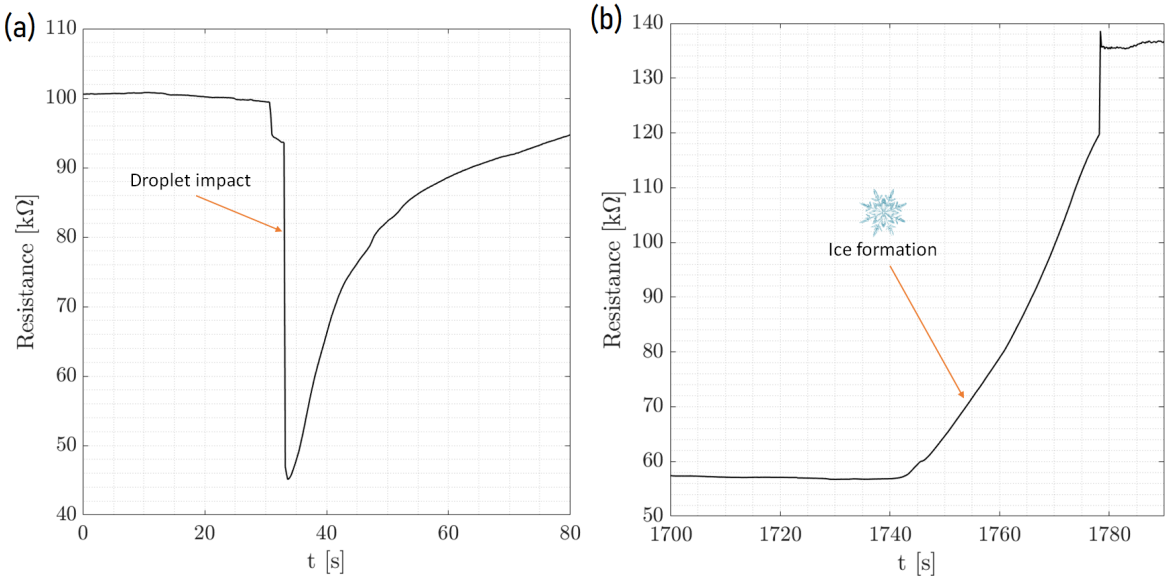

Figure 6. Temperature-controlled chamber experiment. (a) Single drop (Zoom). T_{cold} = -25°C, $T_{chamber}$ = 15°C. (b) Ice formation

 doi:10.20944/preprints202403.1444.v1

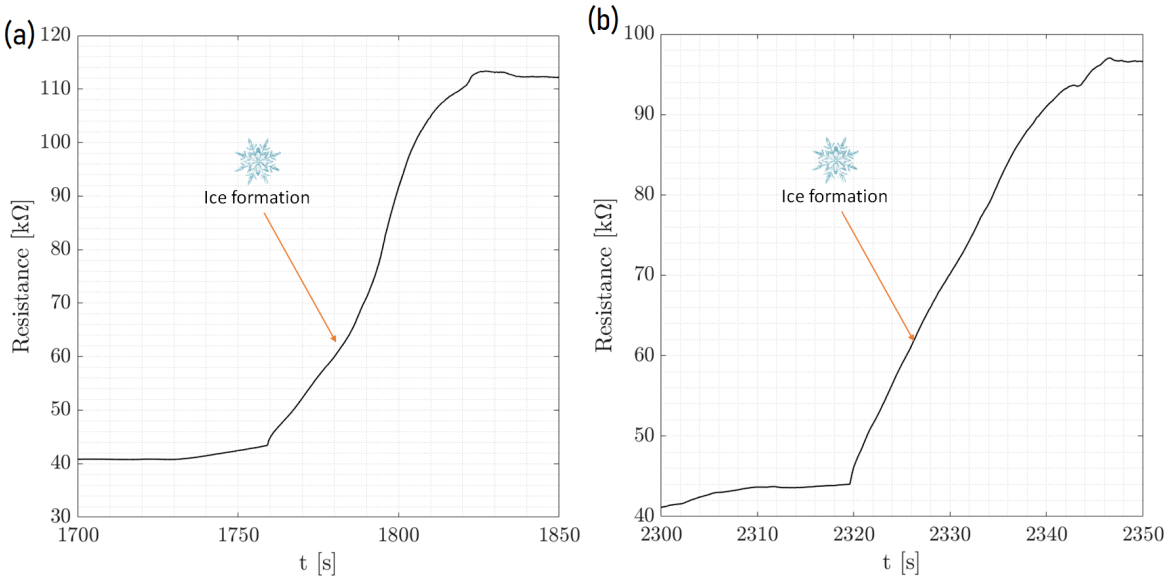

Figure 7. Temperature-controlled chamber experiment. Single drop (Zoom). (a) T_{cold} = -20°C, $T_{chamber}$ = 15°C. (b) T_{cold} = -15°C, $T_{chamber}$ = 15°C.

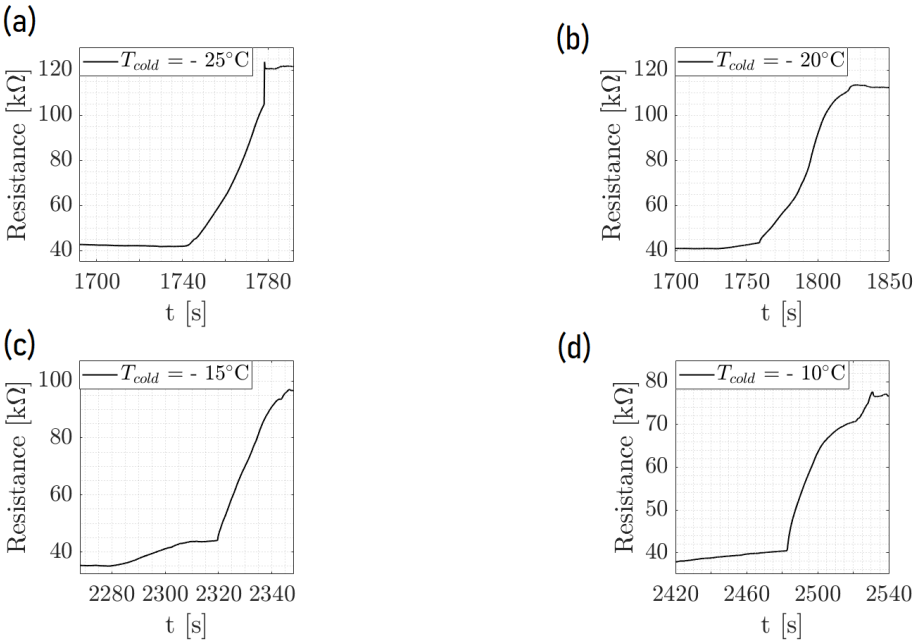

Figure 8. Temperature-controlled chamber experiment with $T_{chamber}$ = 15°C, illustrating the resistance change due to ice formation at a fixed chamber temperature of 15°C. Subfigures (a), (b), (c), and (d) demonstrate the sensor's response over time at various cold junction temperatures: (a) -25°C, (b) -20°C, (c) -15°C, and (d) -10°C, respectively. The sharp increase in resistance indicates the onset of ice formation on the sensor surface.

Table 2. Ice signals amplitudes comparison.

T_{cold} (°C)	ΔR_{ICE} (kΩ)
-25	82
-20	70
-15	52
-10	37

 doi:10.20944/preprints202403.1444.v1

Furthermore, Figure 9 shows the resistance behavior of an ice detection sensor during phase change within the environmental chamber, demonstrating the effect of ambient temperature on the amplitude of the ice signal. As the chamber's temperature is systematically lowered, the amplitude of the resistance signal increases, which is indicative of the enhanced sensitivity of the sensor to the phase change at colder ambient temperatures. This implies that the colder the chamber keeping the same temperature of the droplet and plate for the cycles, the more distinct the resistance change, which is critical for precise ice detection. The comparison between the two graphs at different chamber temperatures (15°C and 10°C) highlights the sensor's response to environmental changes, reinforcing the importance of temperature control in the calibration and operation of ice detection systems. This analysis confirms the sensor's reliability and its potential application in environments where temperature variations play a crucial role in the formation of ice.

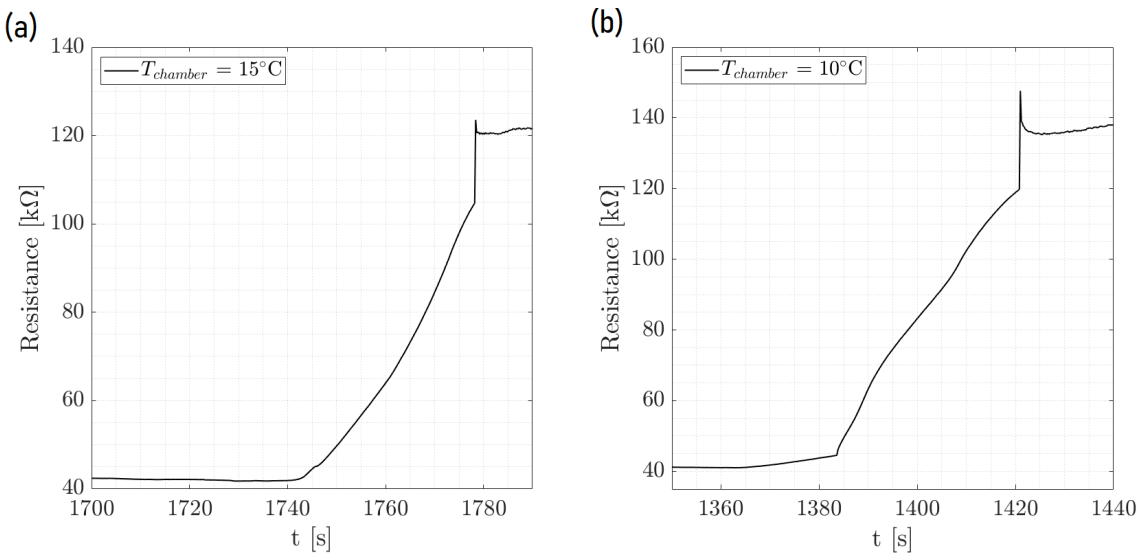

Figure 9. Response of ice detection sensor at (a)$T_{chamber} = 15°C$ and (b) $T_{chamber} = 10°C$, with at $T_{cold} = -20°C$.

Another relevant remark concerns the signals obtained at the injection of the water. A correlation can be observed between the amplitude of the signals and the minimum Peltier temperature, as shown in Figure 10. In particular, as reported in Table 3, the amplitude of the resistance drop is greater when T_{cold} is lower. In Table 3 ΔR_{water} is defined as the difference between the final and the initial values of the resistances respectively after and before injection. Therefore, the modulus has been considered since ΔR_{water} is always negative by definition. The reason is that the resistance R and the temperature T are inversely proportional quantities. As a consequence, when the temperature is lower, the value of the resistance before the injection is higher and therefore, the amplitude is bigger. Either way, a minimum value exists below which the resistance cannot drop, shown in Figure 10 to be around 40 kΩ.

It can also be observed that after the injection signal, the resistance tends to increase with a rate that is higher at lower temperatures, because of the intrinsic behavior of the PEDOT.

Table 3. Water signals amplitudes comparison

T_{cold} (°C)	$\lvert\Delta R_{\text{WATER}}\rvert$ (kΩ)
-25	54
-20	38
-15	23
-10	18

 doi:10.20944/preprints202403.1444.v1

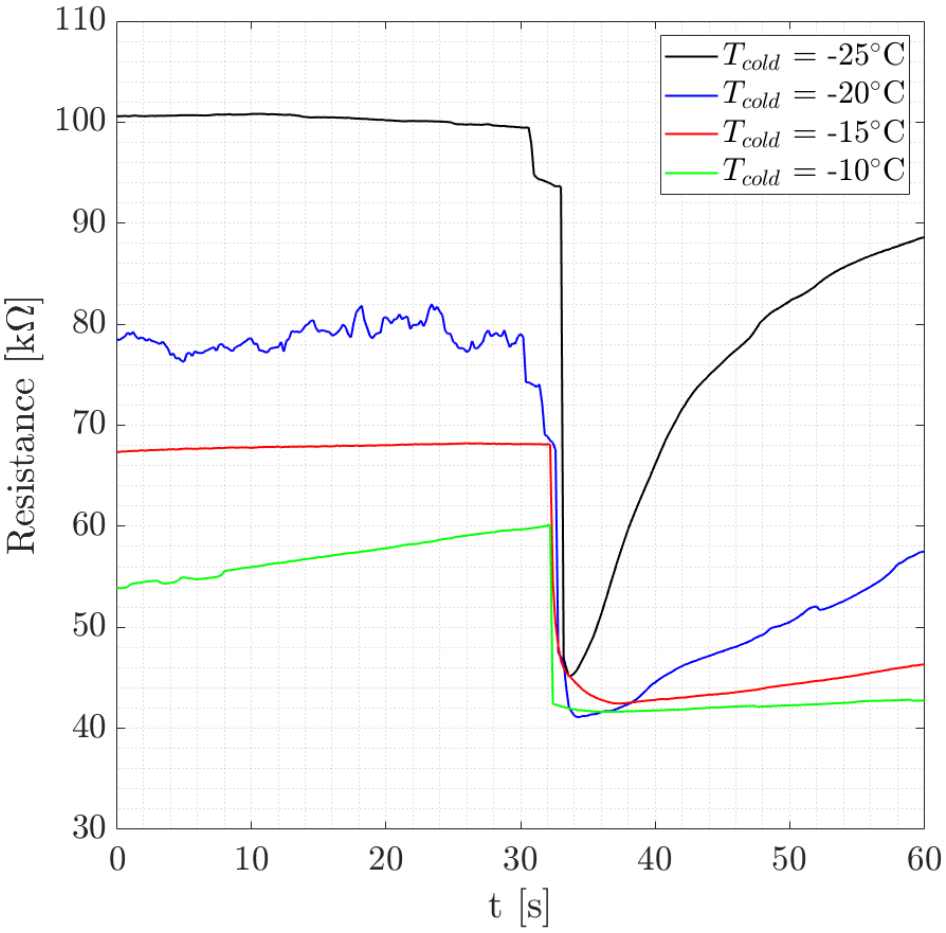

Figure 10. Sensor resistance behavior at different T_{cold} levels, with $T_{chamber}$ = 15 °C.

4. Conclusions and Discussion

In this study, a graphene-based sensor is developed to enhance the detection of ice formation. Utilizing an environmental chamber, we systematically varied environmental conditions such as temperature and humidity. The sensor response to these changes was meticulously recorded, and the resistance behavior was analyzed, indicating phase transitions from the liquid to the solid states. This methodical approach allowed us to explore the potential of the sensor for real-time ice detection in various applications. The observed increase in ice signals amplitude with decreasing minimum temperature, and the associated effects of chamber temperature, underscores the sensor's sensitivity to environmental conditions. This sensitivity is critical in applications where accurate ice detection is paramount, such as in aviation and climate research. The study suggests a strong correlation between the amplitude of ice signals in our sensor and the phase change properties of water under varying thermal conditions. As the chamber temperature decreases, the resistance before droplet injection is higher, leading to more pronounced changes upon freezing.

The signal behavior can be summarized as follows:

- When a droplet touches the sensing element (PEDOT:PSS) of the detector, there is a drop in the internal resistance of the test samples
- A steep increase in resistance occurs when the absorbed water freezes, obstructing the passage of electric charges through the graphene strips due to the formation of ice crystals inside the PEDOT
- An abrupt drop in resistance occurs when the ice melts at a positive local temperature, resulting in a signal similar to the one acquired at the injection. Both signals are classified as "Water" signals.

Our research focuses on testing graphene-based sensors in an environmental chamber, which simulates a variety of climatic conditions that an aircraft could experience during flight. The results

 doi:10.20944/preprints202403.1444.v1

indicate that the developed sensors exhibit heightened sensitivity and rapid response to subtle changes in environmental conditions, especially the critical phase transition from water to ice. This sensitivity is crucial for detecting ice formation at its onset, which is essential for aviation safety. In terms of durability, a few studies have evaluated the long-term performance of graphene-based sensors. One study found that the graphene sensors showed no loss of sensitivity after being exposed to harsh conditions, indicating their potential for long-term use in aviation. However, more studies are needed to evaluate the durability of these sensors in comparison to other alternatives. In terms of cost-effectiveness, the cost of graphene-based sensors is relatively higher than traditional sensors. However, the lightweight, efficient, and highly responsive nature of the graphene sensors makes them a superior alternative to traditional ice detection technologies, which could ultimately reduce costs associated with aircraft maintenance and safety. This research significantly contributes to the field of micromachines by pioneering the application of graphene and PEDOT:PSS-based sensors for ice detection in aviation. It introduces a novel approach that enhances the sensitivity, reliability, and efficiency of ice detection technologies. By leveraging the unique properties of graphene and PEDOT:PSS, the study not only addresses a critical safety concern in aviation but also opens avenues for the development of lightweight, high-performance micromachines with broad implications across various industries. In conclusion, this study reveals graphene-based sensors' broad applicability and transformative potential in detecting ice formation across multiple sectors. Beyond enhancing aviation safety, these sensors can significantly impact wind turbine efficiency by preventing ice accumulation, improving road safety by early ice detection, and supporting maritime navigation and agriculture by mitigating ice and frost risks. This wide range of applications underscores the innovative and versatile solutions graphene-based sensors offer to industries confronting challenges related to ice formation.

Future investigations could explore the optimization of sensor materials to extend the lower threshold of detection, enhancing the sensitivity and range of operation. Additionally, the integration of these sensors with real-time data analysis and machine learning could predict icing events, allowing preemptive actions to be taken in industrial and aeronautical applications. Such advances could lead to more efficient de-icing systems, reduced material wear from ice accumulation, and improved overall safety.

5. Patents

International patent n° WO2022162068A1 / EP4036565A1

Author Contributions: Conceptualization, C.S.I. and D.F.; methodology, D.F.; software, P.Q.; validation, H.M., C.S.I. and D.F.; formal analysis, M.M.; investigation, D.F., M.M.; resources, D.F., M.M.; data curation, D.F., M.M.; writing—original draft preparation, D.F., M.M., and H.M.; writing—review and editing, D.F., M.M., C.S.I and H.M.; visualization, D.F., M.M., and P.Q.; supervision, C.S.I.; project administration, C.S.I.; funding acquisition, C.S.I. All authors have read and agreed to the published version of the manuscript.

Funding: This study was conducted within the scope of the Graphene Flagship Spearhead project GICE: Graphene-Based Heater Mat for Electrothermal Ice Protection System. The Graphene Flagship represents a Future and Emerging Technology research endeavor supported by the European Commission.

Data Availability Statement: All system protocols are publicly accessible and can be found at the Université Libre de Bruxelles.

Acknowledgments: This investigation followed preliminary feasibility analyses and the development of novel technology. Special acknowledgment is extended to Dr. Patrice Desiré Dongo as the co-creator of the technology examined in this document.

Conflicts of Interest: The authors declare no conflict of interest. The funders had no role in the design of the study; in the collection, analyses, or interpretation of data; in the writing of the manuscript; or in the decision to publish the results.

Abbreviations

The following abbreviations are used in this manuscript:

ATM	Aero-Thermo-Mechanics
ULB	Université Libre de Bruxelles
CREST	Centre for Research and Engineering in Space Technologies
GOPS	(3-glycidyloxypropyl)trimethoxysilane
PEDOT	Poly(3,4-ethylenedioxythiophene)
PSS	Poly(styrenesulfonate)
PVDF	Polyvinylidene fluoride or polyvinylidene difluoride
LMS	Least Mean Squares
MEMS	micro electro-mechanical systems

References

1. LIU, X.; Liang, H.; ZONG, H.; XIE, L.; SU, Z. Experimental investigation on de-icing by an array of impact rod-type plasma synthetic jets. *Plasma Sci. Technol.* **2023**, *25*, https://doi.org/10.1088/2058-6272/ac9345.
2. Farahani, E.; Liberati, A. C.; Moreau, C.; Dolatabadi, A.; Stoyanov, P. Comparative Evaluation of the Shear Adhesion Strength of Ice on PTFE Solid Lubricant. *Lubricants* **2023**, *11*, https://doi.org/10.3390/lubricants11030105.
3. Lam, J. K.-W.; Hetherington, J. I.; Carpenter, M. D. Ice growth in aviation jet fuel. In *Airbus Operations Limited*, New Filton House, Filton, Bristol BS99 7AR, UK; Cranfield Defence and Security, Cranfield University, Shrivenham, Swindon SN6 8LA, UK; 2012; pp. Received 16 May 2012, Revised 11 May 2013, Accepted 16 May 2013, Available online 9 June 2013. https://doi.org/10.1016/j.fuel.2013.05.048.
4. Kelleher, M.L.; McLemore, C.; Lee, D.; Dávila-Rodríguez, J.; Diddams, S.; Quinlan, F. Compact, Portable, Thermal-Noise-Limited Optical Cavity with Low Acceleration Sensitivity. *Opt. Express* **2023**, https://doi.org/10.1364/oe.486087.
5. Li, J.; Ding, Y.; Liu, X.; Yuan, G.; Cai, Y. Achromatic and Athermal Design of Aerial Catadioptric Optical Systems by Efficient Optimization of Materials. *Sensors (Basel, Switzerland)* **2023**, *23*, https://doi.org/10.3390/s23041754.
6. Lam, J. K.-W.; Hetherington, J. I.; Carpenter, M. D. Ice growth in aviation jet fuel. *Fuel* **2013**, *113*, 402-406. https://doi.org/10.1016/j.fuel.2013.05.048. Available online at https://www.sciencedirect.com/science/article/pii/S0016236113004602.
7. Dongo, P. D.; Hakansson, A.; Stoeckel, M.-A.; Pavlopoulou, E.; Wang, S.; Farina, D.; Queeckers, P.; Fabiano, S.; Iorio, C. S.; Crispin, R. Detection of Ice Formation With the Polymeric Mixed Ionic-Electronic Conductor PEDOT: PSS for Aeronautics. *Advanced Electronic Materials* **2023**, *First published: 20 October 2023*, https://doi.org/10.1002/aelm.202300060. Available online at https://onlinelibrary.wiley.com/doi/10.1002/aelm.202300060.
8. DONGO, Patrice D.; Machrafi, Hatim; Minetti, C.; Amato, Alessandro; Queeckers, P.; Iorio, C.S. A heat-pulse method for detecting ice formation on surfaces. *Thermal Science and Engineering Progress* **2021**, *22*, 100813, doi:https://doi.org/10.1016/j.tsep.2020.100813.
9. Farina, D.; Mazio, M.; Machrafi, H.; Queeckers, P.; Iorio, C.S. Wind Tunnel Characterization of a Graphene-Enhanced PEDOT:PSS Sensing Element for Aircraft Ice Detection Systems. *Micromachines (Basel)* **2024**, *15*(2), 198. https://doi.org/10.3390/mi15020198. PMID: 38398926; PMCID: PMC10891575.
10. Ting Ma, Sensen Zhu, Zihang Ge, Fangyi Wan, Chunlin Zhang, Guanghui Liu. Aircraft sensor fault detection based on SLD-LMS algorithm. *2022 Prognostics and Health Management Conference (PHM-2022 London)*. 2022, , 247-250. https://doi.org/10.1109/PHM2022-London52454.2022.00051.
11. H. Hua, Zhen Zhang, Huachen Feng. Research Status and Method of Aviation Sensor Performance Evaluation. *Journal of Physics: Conference Series*. 2021, 1769. https://doi.org/10.1088/1742-6596/1769/1/012050.
12. Varadan, V. K., & Varadan, V. V. (2000). Microsensors, microelectromechanical systems (MEMS), and electronics for smart structures and systems. Smart Materials and Structures, 9(6), 953. doi: 10.1088/0964-1726/9/6/327
13. Strijhak, S., Ryazanov, D., Koshelev, K., & Ivanov, A. (2022). Neural Network Prediction for Ice Shapes on Airfoils Using iceFoam Simulations. Aerospace, 9, 96. https://doi.org/10.3390/aerospace9020096.

14. M. Homola, P. J. Nicklasson, P. Sundsbø. Ice sensors for wind turbines. *Cold Regions Science and Technology*. 2006, 46, 125-131. https://doi.org/10.1016/J.COLDREGIONS.2006.06.005.
15. Yihua Cao, Wenyuan Tan, Zhenlong Wu. Aircraft icing: an ongoing threat to aviation safety. *Aerospace Science and Technology*. 2018, 75, 353-385. https://doi.org/10.1016/J.AST.2017.12.028.
16. Håkansson, A.; Han, S.; Wang, S.; Lu, J.; Braun, S.; Fahlman, M.; Berggren, M.; Crispin, X.; Fabiano, S. Effect of (3-glycidyloxypropyl)trimethoxysilane (GOPS) on the electrical properties of PEDOT:PSS films. *Journal Name Here* **2017**, *First published: 10 March 2017*, https://doi.org/10.1002/polb.24331. Available online at https://doi.org/10.1002/polb.24331.
17. MITRAKA, E.; Jafari, M. J.; Vagin, M.; Liu, X.; Fahlman, M.; Ederth, T.; Berggren, M.; Jonsson, M. P.; Crispin, X. Oxygen-induced doping on reduced PEDOT. *J. Mater. Chem. A* **2017**, *5*(9), 4404-4412, https://doi.org/10.1039/C6TA10521A.
18. AHMED, Fareed; Ding, Penghui; Ail, Ujwala; Warczak, Magdalena; Grimoldi, Andrea; Ederth, Thomas; Håkansson, Karl M.O.; Vagin, Mikhail; Gueskine, Viktor; Berggren, Magnus; Crispin, Xavier. Manufacturing Poly(3,4-Ethylenedioxythiophene) Electrocatalytic Sheets for Large-Scale H2O2 Production. *Advanced Sustainable Systems* **2021**, https://doi.org/10.1002/adsu.202100316.
19. Huang, X.; Zeng, Z.; Fan, Z.; Liu, J.; Zhang, H. Graphene-Based Electrodes. *Advanced Materials* **2012**, *24*(45), 5979-6004, doi:https://doi.org/10.1002/adma.201201587.
20. Sibilia, S.; Tari, L.; Bertocchi, F.; Chiodini, S.; Maffucci, A. A Capacitive Ice-Sensor Based on Graphene Nano-Platelets Strips. *Sensors* **2023**, *23*, 9877. https://doi.org/10.3390/s23249877.